# Detection of Diethyl Ether by a Europium MOF through Fluorescence Enhancement①

WANG Xue-Ting[a, b] WEI Wei[b]
ZHANG Kai[b] DU Shao-Wu[a, b②]

[a] (*Fujian Key Laboratory of Functional Marine Sensing Materials, Minjiang University, Fuzhou* 350108, *China*)

[b] (*State Key Laboratory of Structural Chemistry, Fujian Institute of Research on the Structure of Matter, Chinese Academy of Sciences, Fuzhou* 350002, *China*)

**ABSTRACT** A new water-stable europium MOF, $(Me_2NH_2)$[Eu(abtc)(phen)] $2H_2O$ (**1**), has been synthesized from $Eu(NO_3)_3$ $6H_2O$ with 1,10-phenanthroline (phen) and 3,3′,5,5′-azobenzenetetracarboxylic acid ($H_4$abtc) ligands under solvothermal conditions and structurally characterized by single-crystal X-ray diffraction analysis, IR, TGA and PXRD. It crystallizes in monoclinic system, *C*2/*c* space group, with *a* = 16.278(3), *b* = 14.261(3), *c* = 27.936(5) Å, $\beta$ = 103.464(3)°, *V* = 6307(2) Å$^3$, *Z* = 8, $C_{30}H_{26}EuN_5O_{10}$, $M_r$ = 768.5, $D_c$ = 1.543 g/cm$^3$, *F*(000) = 2912, $\mu$(Mo*Ka*) = 2.044 mm$^{-1}$, *R* = 0.0315 and *wR* = 0.0663. In the structure of **1**, the $EuO_7N_2$ polyhedra are assembled into a 2*D* layer with rhombic windows and these layers are further condensed to form a 3*D* framework. It can be used as selective and sensitive fluorescence sensors capable of detecting diethyl ether vapor.

**Keywords: lanthanide MOF, water stable, fluorescence enhancement, diethyl ether detection;**
**DOI: 10.14102/j.cnki.0254–5861.2011–2917**

## 1 INTRODUCTION

Recognition and detection of small organic molecules have drawn more and more attention because of their important impact on environment[1-3]. Volatile organic solvents, in particular, are highly toxic and can thus affect environment and human body more widely. Hence, there is a strong need to develop a quick response and simple identification method for the volatile organic solvents. Fluorescence recognition has received much attention because of its short response time, excellent sensitivity and simplicity[4]. This technique has been applied to detect small organic molecules such as explosives, amines and acetonitrile[5-11].

Lanthanide metal-organic frameworks (Ln-MOFs), a new class of crystalline luminescence materials, have been of great importance due to their high luminescence efficiency, large Stokes shifts, narrow band emissions and long luminescence lifetimes[12]. Ln-MOFs with high luminescence intensity can be rationally designed and synthesized *via* the appropriate choice of antenna ligands and $Ln^{3+}$ ions[13-16]. Owing to the electron (charge) transfer processes, the interaction of analytes to be tested with Ln-MOFs may alter the luminescence intensity, hence resulting in their emission color changes. Taking advantages of the obvious emission color changes, Ln-MOFs are able to probe small organic molecules, including organic solvents, dyes, explosives and antibiotics[17-19]. However, for the detection of organic solvents, most are performed in liquid phase. Detection of organic solvent vapor by Ln-MOFs is less common. Herein, considering that both 3,3′,5,5′-azobenzenetetracarboxylic acid ($H_4$abtc) bearing a photochromic azo group and 1,10-phenanthroline (phen) are strong light-harvesting organic chromophores and are beneficial to improve the luminescence properties of Ln-MOFs, we used them as a bridging and a chelating ligands, respectively, to construct an Eu-MOF, formulated as $(Me_2NH_2)$[Eu(abtc)(phen)] $2H_2O$ (**1**). Compound **1** was fully characterized by elemental analysis, IR, TGA, and PXRD. It has good thermal stability and is also stable in aqueous solution. Moreover, **1** was found to be a selective and sensitive fluorescent probe for diethyl ether in solution or vapor state. It is worth mentioning that this is the first report for detecting diethyl ether vapor using Ln-MOFs

Received 23 June 2020; accepted 1 September 2020 (**CCDC 1974179**)

① This work was supported by the National Natural Science Foundation of China (21972060)

② Corresponding author. E-mail: swdu@fjirsm.ac.cn

through a luminescence enhancement mechanism.

## 2 EXPERIMENTAL

### 2. 1 Materials and physical measurements

All reagents were commercially purchased and used without further purification. Elemental analyses (C, H, and N) were carried out using an elemental Vario EL III analyzer. Experimental powder X-ray diffraction (PXRD) was recorded on a Miniflex 600 diffractometer with Cu*Ka* radiation ($\lambda$ = 1.5406 Å) at a scan speed of 1.6 °/min. Thermogravimetric analysis (TGA) was measured on an TGA/NETZSCH STA 449C analyzer at a heating rate of 10 ℃/min under nitrogen atmosphere. Infrared spectrum was recorded on a PerkinElmer Spectrum-One spectrophotometer using the KBr pellet. The emission spectra were obtained on an Edinburgh FLS fluorescence spectrophotometer.

### 2. 2 Synthesis of $(Me_2NH_2)[Eu(abtc)(phen)]\cdot 2H_2O$

A mixture of $Eu(NO_3)_3\cdot 6H_2O$ (0.1 mmol), 3,3′,5,5′-azobenzenetetracarboxylic acid ($H_4$abtc, 0.05 mmol), phen (0.1 mmol), $H_2O$ (1 mL), and DMA (5 mL) was placed in a 25 mL Teflon cup and heated at 150 ℃ for 2 days. Then, the reaction was slowly cooled down to room temperature to obtain orange block crystals. After filtration, the product was washed with ethanol and air-dried. Yield: 165 mg, 73% (based on Eu). Elemental analysis (%): calcd. for **1**: $C_{30}H_{26}N_5O_{10}Eu$ (768.50): C, 46.84; H, 3.38; N, 9.11. Found (%): C, 46.65; H, 3.13, N, 9.46. IR ($cm^{-1}$): 1610 (vs), 1552 (s), 1437 (s), 1373 (vs), 1239 (w), 1145 (w), 1092 (m), 1015 (w), 932 (w), 855 (m), 798 (m), 721 (s), 625 (w), 490 (w), 465 (w), 420 (w).

### 2. 3 X-ray crystallographic study

Single-crystal X-ray diffraction data for **1** were collected on a Rigaku Mercury CCD diffractometer equipped with graphite-monochromated Mo*Kα* radiation ($\lambda$ = 0.71073 Å) at 293(2) K. Absorption correction was carried out by the multi-scan program. The structure was solved by direct methods with SHELXS-97[20] and refined by the full-matrix least-squares method on $F^2$ using the SHELXL-2016 program[21]. The contribution from disordered guest solvents was removed by using the SQUEEZE program implemented in PLATON[22]. Selected bond lengths and bond angles are listed in Table 1. Crystallographic data have been deposited at the Cambridge Crystallographic Data Center.

**Table 1. Selected Bond Lengths (Å) and Bond Angles (°) for Compound 1**

| Bond | Dist. | Bond | Dist. | Bond | Dist. |
|---|---|---|---|---|---|
| Eu(1)–O(1) | 2.469(3) | Eu(1)–O(5) | 2.483(3) | Eu(1)–O(8)$^b$ | 2.394(3) |
| Eu(1)–O(2) | 2.558(3) | Eu(1)–O(6) | 2.572(3) | Eu(1)–N(3) | 2.625(4) |
| Eu(1)–O(4)$^a$ | 2.417(3) | Eu(1)–O(7) | 2.354(2) | Eu(1)–N(4) | 2.593(3) |
| Angle | (°) | Angle | (°) | Angle | (°) |
| O(1)–Eu(1)–O(2) | 52.04(8) | O(7)–Eu(1)–O(6) | 71.71(8) | O(5)–Eu(1)–O(6) | 51.87(8) |
| O(1)–Eu(1)–O(5) | 78.74(9) | O(7)–Eu(1)–N(3) | 83.18(11) | O(5)–Eu(1)–N(4) | 82.49(10) |
| O(1)–Eu(1)–N(3) | 146.08(10) | O(8)$^b$–Eu(1)–O(1) | 76.27(9) | O(6)–Eu(1)–N(4) | 130.55(10) |
| O(2)–Eu(1)–O(6) | 104.98(9) | O(8)$^b$–Eu(1)–O(4)$^a$ | 137.39(10) | O(7)–Eu(1)–O(2) | 135.94(9) |
| O(2)–Eu(1)–N(4) | 70.72(10) | O(8)$^b$–Eu(1)–O(6) | 136.92(8) | O(7)–Eu(1)–O(5) | 123.44(9) |
| O(4)$^a$–Eu(1)–O(2) | 134.55(9) | O(8)$^b$–Eu(1)–N(4) | 90.79(10) | O(7)–Eu(1)–O(8)$^b$ | 79.66(9) |
| O(4)$^a$–Eu(1)–O(6) | 73.77(9) | O(1)–Eu(1)–O(6) | 71.15(9) | O(7)–Eu(1)–N(4) | 145.15(11) |
| O(5)–Eu(1)–O(2) | 70.90(9) | O(1)–Eu(1)–N(4) | 122.76(10) | O(8)$^b$–Eu(1)–O(2) | 74.44(9) |
| O(5)–Eu(1)–N(3) | 132.83(10) | O(2)–Eu(1)–N(3) | 118.98(11) | O(8)$^b$–Eu(1)–O(5) | 144.99(9) |
| O(6)–Eu(1)–N(3) | 134.73(10) | O(4)$^a$–Eu(1)–O(1) | 144.23(10) | O(8)$^b$–Eu(1)–N(3) | 69.98(10) |
| O(7)–Eu(1)–O(1) | 87.65(9) | O(4)$^a$–Eu(1)–O(5) | 74.32(10) | N(3)–Eu(1)–N(4) | 62.13(12) |
| O(7)–Eu(1)–O(4)$^a$ | 87.94(9) | O(4)$^a$–Eu(1)–N(3) | 68.14(11) | | |

Symmetry transformation: a: $x$ + 1/2, $y$ + 1/2, $z$; b: –$x$ + 1, –$y$, –$z$

## 3 RESULTS AND DISCUSSION

### 3. 1 Structure description

Single-crystal X-ray diffraction analysis reveals that **1** crystallizes in the monoclinic system, *C*2/*c* space group. The SQUEEZE function in PLATON was used during the refinement due to the highly disordered solvents. TGA and elemental analyses indicate the presence of two free water molecules. The asymmetric unit of **1** consists of one crystallographically independent $Eu^{3+}$ ion, one $abtc^{4-}$ ligand, one phen ligand, one protonated dimethylamine cation and two free water molecules. As shown in Fig. 1, the

nine-coordinated environment of $Eu^{3+}$ is fulfilled by seven carboxylate oxygen atoms derived from the $abtc^{4-}$ ligands and two nitrogen atoms from a phen ligand. The Eu–O bond lengths range from 2.356(4) to 2.573(4) Á and the Eu–N bond lengths are 2.595(5) and 2.620(5) Å. The O–Eu–O bond angles range from 51.89(11) to 144.20(13) ° and the N–Eu–N bond angle is 62.12(17) °, all of which are comparable to those reported in the related $Eu^{3+}$ compounds[23]. The four carboxylate groups of the $H_4$abtc ligand are all deprotonated and adopt three types of bridging modes: ($\kappa^1$-$\kappa^1$)-$\mu_1$, $\kappa^1$-$\mu_1$ and ($\kappa^1$-$\kappa^1$)-$\mu_2$. Each $abtc^{4-}$ ligand acts as a $\mu_5$-bridge to link five $Eu^{3+}$ ions (Fig. 1). In the structure of **1**, two symmetry-related $EuO_7N_2$ polyhedra are assembled into a dimer by bridging carboxylate groups with the Eu ··Eu distance of 5.8097 Å, and these dimers are linked by bridging $abtc^{4-}$ ligands to form a 2*D* layer with rhombic windows (Fig. 2). Then a 3*D* framework of **1** is formed from these 2*D* layers *via* the linkage of $abtc^{4-}$ ligands (Fig. 3). Unlike most lanthanide-abtc frameworks where the $Ln^{3+}$ centers are usually seven- or eight-coordinate and their coordination spheres are fulfilled by one or two terminally coordinated solvent molecules, such as $H_2O$, DMF, DMA and DMSO, the $Eu^{3+}$ center in **1**, as also observed in its most related Tb-abtc compound, adopts a distorted tricapped trigonal prism geometry and is nine-coordinate without any coordinated solvent molecules[24-26]. Furthermore, the coordination sphere of $Eu^{3+}$ ion is completed by a chelating phen ligand, which plays an important role in the enhancement of stability.

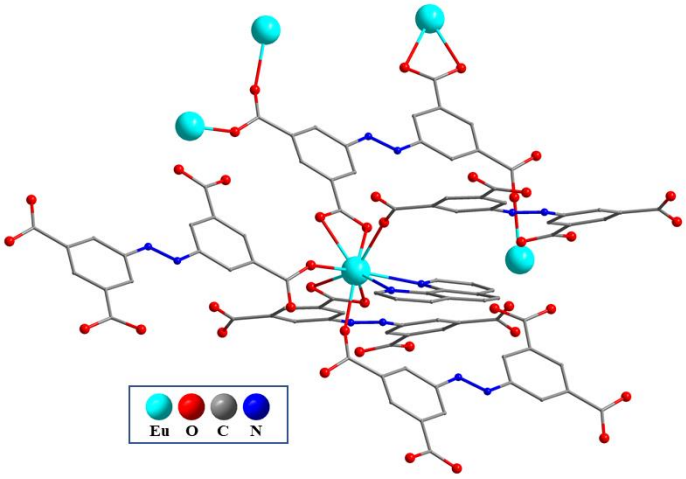


**Fig. 1. Coordination environment of $Eu^{3+}$ ion and coordination mode of the ligand in 1**

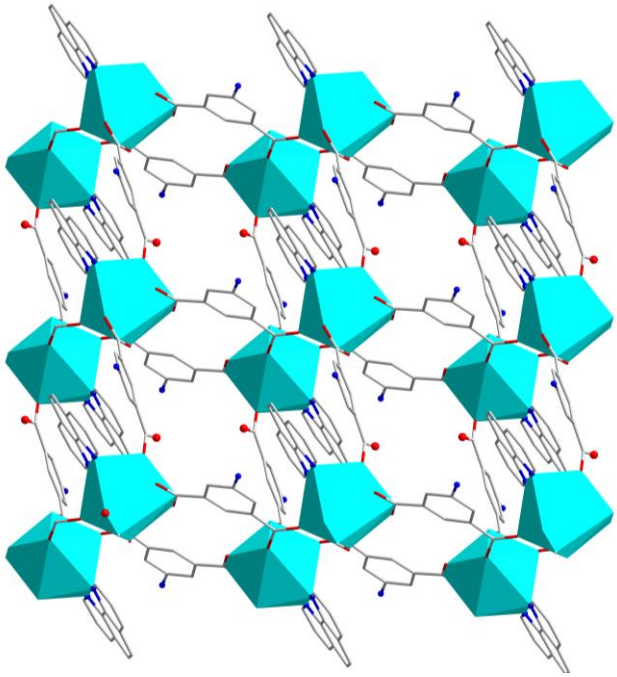

**Fig. 2. View of 2*D* layer of compound 1**

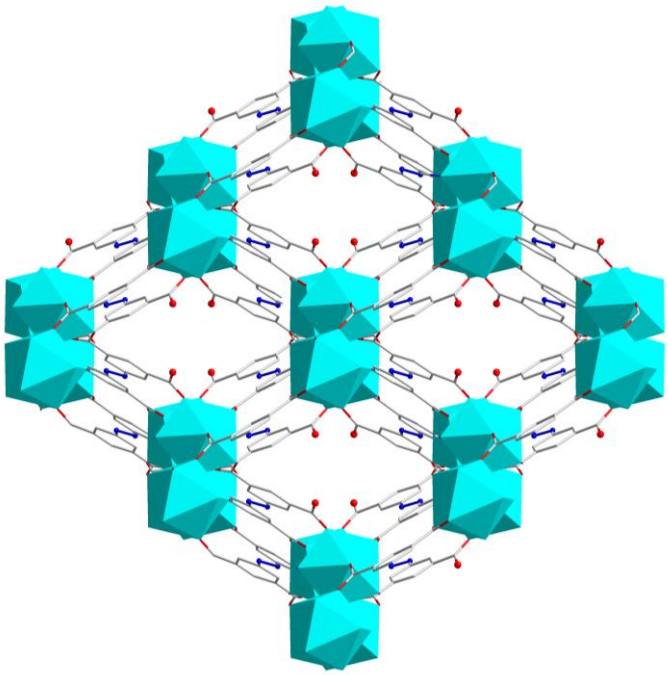

**Fig. 3. View of 3*D* framework of compound 1. The phen ligands are omitted for clarity**

### 3. 2 Chemical and thermal stability of 1

To confirm the phase purity, the powder X-ray diffraction of **1** was measured at room temperature. The diffraction pattern is consistent with the simulated one based on the single-crystal X-ray diffraction, implying phase purity of the as-synthesized sample (Fig. 4). Furthermore, the acid stability of **1** was tested by soaking the sample in aqueous solutions of various pH values (3 to 11) for one day. The XRD results showed that after soaking, the patterns of XRD remained the same, which indicated that there was no structural change. TGA result shows that the first weight loss from 30 to 160 ℃ with the loss of 4.91% is due to the departure of lattice water (calcd. 4.68%) (Fig. 5). The second weight loss from 160 to 340 ℃ with the loss of 5.47% is due to the removal of $Me_2NH_2$ cation (calcd. 5.99%). Further increase in temperature leads to the framework decomposition.

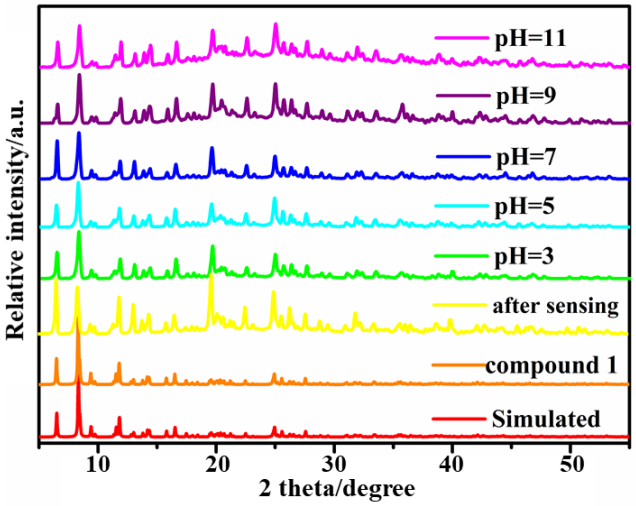


**Fig. 4. PXRD patterns of 1 after immersion in aqueous solutions with pH ranging from 3 to 11 and after sensing**

### 3. 3 Fluorescence sensing

The solid-state fluorescence of **1** was recorded. Upon excitation at 290 nm, the emission spectrum consists of four peaks at 594, 614, 652 and 700 nm due to the $^5D_0 \rightarrow {}^7F_J$ ($J$ =

1, 2, 3, 4) transition of $Eu^{3+}$. The peak at 614 nm results from the hypersensitive transition $^5D_0 \rightarrow {}^7F_2$ of $Eu^{3+}$ and has the maximum intensity.

In recent years, recognition and sensing of small molecules, in particular volatile organic molecules have provoked more and more attention. To probe its potential application as chemical sensor, the fluorescence emission of **1** in a range of common solvents (diethyl ether, water, formaldehyde, ethanol, methylbenzene, acetonitrile, methanol and acetone) was measured. As depicted in Fig. 6a, the emission intensity of **1** varies depending on the types of solvents. Obviously, the fluorescent intensity in diethyl ether increases about 3.4 times than that in water and formaldehyde, while in the rest solvents it decreases more or less. In addition, compound **1** has a good cyclic performance. After five cycles of repetition, the luminescence intensity does not change significantly (Fig. 6b). Therefore, compound **1** might be used for the selective detection of diethyl ether.

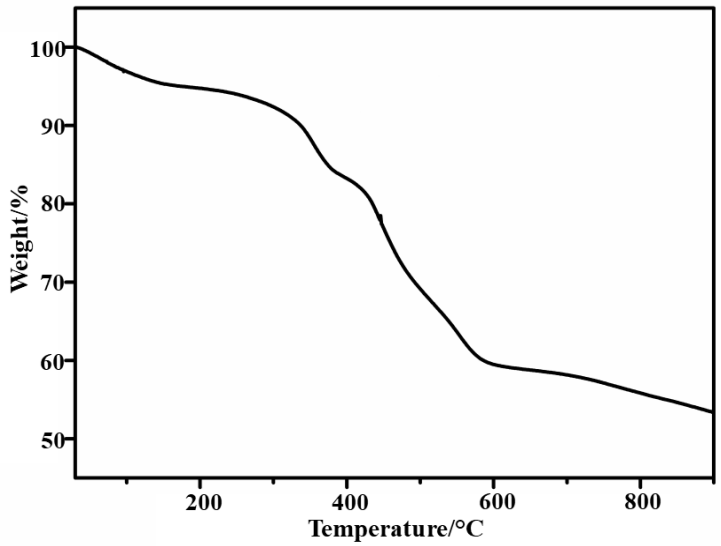


**Fig. 5. TGA curve of compound 1**

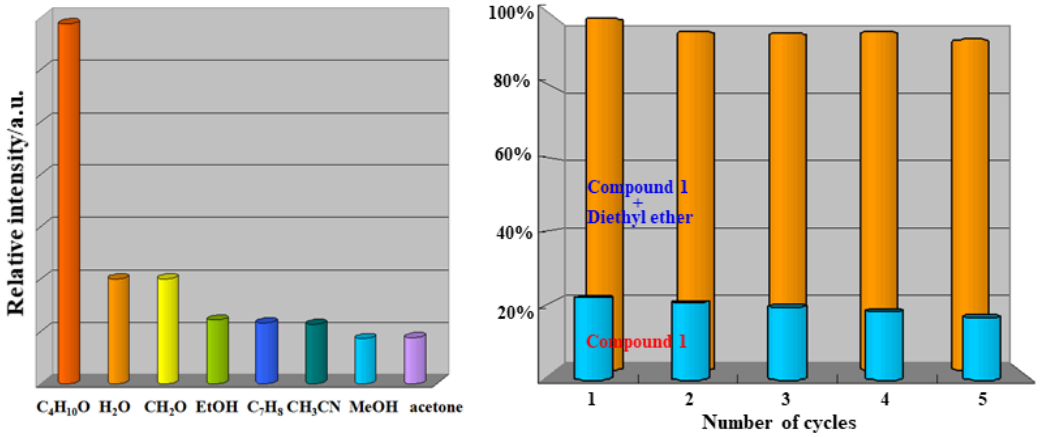


**(a)** **(b)**

**Fig. 6. (a) Luminescence intensity of 1 dispersed in different solvents, (b) Five cycle tests of 1 for sensing diethyl ether**

The fluorescence enhancement of diethyl ether, as well as its good chemical stability, promotes us to study its detection ability for diethyl ether in vapor state. To avoid deterioration of diethyl ether, the sensing experiments were performed under indoor environmental conditions at room temperature. An open sample tube with finely ground sample of **1** was placed in a sealed container, containing diethyl ether (Scheme 1). The time-dependent fluorescent intensity of **1** shows a continuous enhancement upon exposure to diethyl ether vapor for 10, 30, 45 and 60 min (Fig. 7). The fluorescence enhancement efficiency reaches to a maximum in 60 min. These experimental results indicate that **1** could be a promising chemical sensor for detecting diethyl ether vapors.

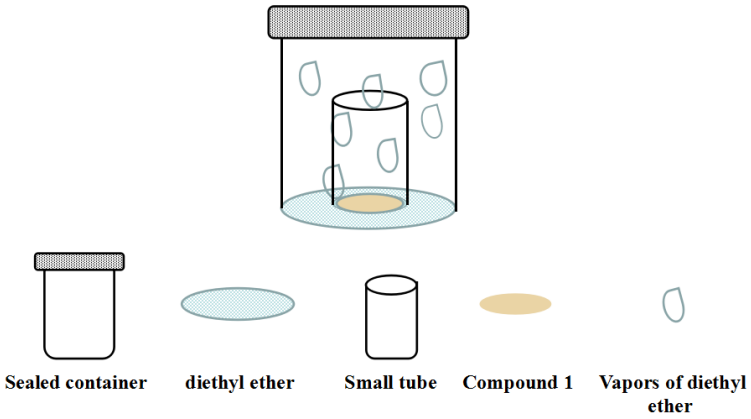


**Scheme 1. Diagram of sensing measurements for diethyl ether vapors**

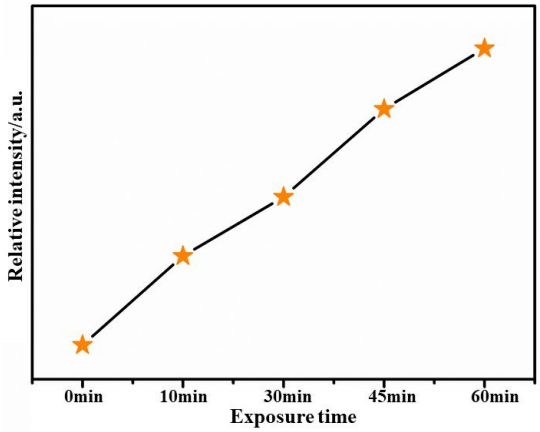


**Fig. 7. Fluorescence efficiency of 1 exposed in diethyl ether vapor for different time**

### 3. 3 Possible mechanism for fluorescence sensing

The mechanism for detection of diethyl ether was further investigated. The PXRD pattern of **1** after sensing test is exactly the same as that of the simulated one, which suggests that the interaction of diethyl ether with **1** does not cause structural collapse. The enhancement of fluorescent intensity may be due to the interaction between diethyl ether and the framework. The presence of diethyl ether may replace some $H_2O$ surrounding the mental center, which can decrease H-bond oscillation, hence resulting in fluorescence enhancement[27, 28].

## 4 CONCLUSION

In summary, we have successfully synthesized **1** *via* self-assembly of $H_4$abtc and phen ligands with $Eu^{3+}$ under solvothermal condition. Compound **1** is a porous 3*D* framework and its application in detection organic solvent molecules was also explored. It displays an obvious fluorescence enhancement effect in diethyl ether. Further study demonstrated that **1** was also capable of detecting diethyl ether vapor.

## REFERENCES

(1) Yi, F. Y.; Yang, W.; Sun, Z. M. Highly selective acetone fluorescent sensors based on microporous Cd(II) metal-organic frameworks. *J. Mater. Chem*. **2012**, 22, 23201−23209.

(2) Zhao, S. S.; Yang, J.; Liu, Y. Y.; Ma, J. F. Fluorescent aromatic tag-functionalized MOFs for highly selective sensing of metal ions and small organic molecules. *Inorg. Chem*. **2016**, 55, 2261−2273.

(3) Ruta, J.; Perrier, S.; Ravelet, C.; Fize, J.; Peyrin, E. Noncompetitive fluorescence polarization aptamer-based assay for small molecule detection. *Anal. Chem*. **2009**, 81, 7468−7473.

(4) Hao, J. N.; Yan, B.; Determination of urinary 1-hydroxypyrene for biomonitoring of human exposure to polycyclic aromatic hydrocarbons carcinogens by a lanthanide-functionalized metal-organic framework sensor. *Adv. Funct. Mater*. **2017**, 27, 1603856−1603863.

(5) Chen, D. M.; Tian, J. Y.; Chen, M.; Liu, C. S.; Du, M. Moisture-stable Zn(II) metal-organic framework as a multifunctional platform for highly efficient $CO_2$ capture and nitro pollutant vapor detection. *ACS Appl. Mater. Interfaces* **2016**, 8, 18043−18050.

(6) Qin, J.; Ma, B.; Liu, X. F.; Lu, H. L.; Dong, X. Y.; Zang, S. Q.; Hou, H. Aqueous- and vapor-phase detection of nitroaromatic explosives by a water-stable fluorescent microporous MOF directed by an ionic liquid. *J. Mater. Chem. A* **2015**, 3, 12690−12697.

(7) Shen, X.; Yan, B. A novel fluorescence probe for sensing organic amine vapors from a $Eu^{3+}$ *β*-diketonate functionalized bio-MOF-1 hybrid system. *J. Mater. Chem. C* **2015**, 3, 7038−7044.

(8) Wang, J. H.; Li, M.; Li, D. A dynamic, luminescent and entangled MOF as a qualitative sensor for volatile organic solvents and a quantitative monitor for acetonitrile vapour. *Chem. Sci*. **2013**, 4, 1793−1801.

(9) Zhan, C.; Ou, S.; Zou, C.; Zhao, M.; Wu, C. D. A luminescent mixed-lanthanide-organic framework sensor for decoding different volatile organic molecules. *Anal. Chem*. **2014**, 86, 6648−6653.

(10) Li, R.; Yuan, Y. P.; Qiu, L. G.; Zhang, W.; Zhu, J. F. A rational self-sacrificing template route to metal-organic framework nanotubes and reversible vapor-phase detection of nitroaromatic explosives. *Small* **2012**, 8, 225−230.

(11) Chen, D. M.; Zhang, N. N.; Liu, C. S.; Du, M. Template-directed synthesis of a luminescent Tb-MOF material for highly selective $Fe^{3+}$ and $Al^{3+}$ ion detection and VOC vapor sensing. *J. Mater. Chem. C* **2017**, 5, 2311−2317.

(12) Pan, Y.; Su, H. Q.; Zhou, E. L.; Yin, H. Z.; Shao, K. Z.; Su, Z. M. A stable mixed lanthanide metal-organic framework for highly sensitive thermometry. *Dalton Trans*. **2019**, 48, 3723−3729.

(13) Chen, Z.; Sun, Y.; Zhang, L.; Sun, D.; Liu, F.; Meng, Q.; Wang, R.; Sun, D. A tubular europium-organic framework exhibiting selective sensing of $Fe^{3+}$ and $Al^{3+}$ over mixed metal ions. *Chem. Commun*. **2013**, 49, 11557−11559.

(14) Wu, Y. P.; Xu, G. W.; Dong, W. W.; Zhao, J.; Li, D. S.; Zhang, J.; Bu, X. Anionic lanthanide MOFs as a platform for iron-selective sensing, systematic color tuning, and efficient nanoparticle catalysis. *Inorg. Chem*. **2017**, 56, 1402−1411.

(15) Zhou, X. H.; Li, L.; Li, H. H.; Li, A.; Yang, T.; Huang, W. A flexible Eu(III)-based metal-organic framework: turn-off luminescent sensor for the detection of Fe(III) and picric acid. *Dalton Trans*. **2013**, 42, 12403−12409.

(16) Li, H.; Han, Y.; Shao, Z.; Li, N.; Huang, C.; Hou, H. Water-stable Eu-MOF fluorescent sensors for trivalent metal ions and nitrobenzene. *Dalton Trans*. **2017**, 46, 12201−12208.

(17) Zhang, Q.; Lei, M.; Yan, H.; Wang, J.; Shi, Y. A water-stable 3*D* luminescent metal-organic framework based on heterometallic $[Eu^{III}_6Zn^{II}]$ clusters showing highly sensitive, selective, and reversible detection of ronidazole. *Inorg. Chem.* **2017**, 56, 7610−7614.

(18) Xu, W.; Chen, H.; Xia, Z.; Ren, C.; Han, J.; Sun, W.; Wei, Q.; Xie, G.; Chen, S. A robust $Tb^{III}$-MOF for ultrasensitive detection of trinitrophenol: matched channel dimensions and strong host-guest interactions. *Inorg. Chem*. **2019**, 58, 8198−8207.

(19) Yang, Y.; Chen, L.; Jiang, F.; Wan, X.; Yu, M.; Cao, Z.; Jing, T.; Hong, M. Fabricating a super stable luminescent chemosensor with multi-stimuli-response to metal ions and small organic molecules by turn-on and turn-off effects. *J. Mater. Chem. C* **2017**, 5, 4511−4519.

(20) Sheldrick, G. M. *SHELXS-97, Program for Crystal Structure Solution*. University of Göttingen, Germany **1997**.

(21) Sheldrick, G. M. Crystal structure refinement with SHELXL. *Acta Crystallogr. Sec. C: Struct. Chem*. **2015**, 71, 3−8.

(22) Spek, A. L. Single-crystal structure validation with the program PLATON. *J. Appl. Cryst*. **2003**, 36, 7−13.

(23) Xu, S.; Shi, J. J.; Ding, B.; Liu, Z. Y.; Wang, X. G.; Zhao, X. J.; Yang, E. C. A heterometallic sodium(I)-europium(III)-organic layer exhibiting dual-responsive luminescent sensing for nitrofuran antibiotics, $Cr_2O_7^{2-}$ and $MnO_4^-$ anions. *Dalton Trans*. **2019**, 48, 1823−1834.

(24) Castells-Gil, J.; Baldov ́ı J. J.; Mart ́ınGastaldo, C.; Espallargas, G. M. Implementation of slow magnetic relaxation in a SIM-MOF through a structural rearrangement. *Dalton Trans*. **2018**, 41, 14734−14740.

(25) Du, P. Y.; Gu, W.; Liu, X. Multifunctional three-dimensional europium metal-organic framework for luminescence sensing of benzaldehyde and $Cu^{2+}$ and selective capture of dye molecules. *Inorg. Chem*. **2016**, 55, 7862−7828.

(26) Goel, N.; Kumar, N. A dual-functional luminescent Tb(III) metal-organic framework for the selective sensing of acetone and TNP in water. *RSC Adv*. **2018**, 8, 10746−10755.

(27) Zheng, K.; Liu, Z. Q.; Huang, Y.; Chen, F.; Zeng, C. H.; Zhong, S.; Ng, S. W. Highly luminescent Ln-MOFs based on 1,3-adamantanediacetic acid as bifunctional sensor. *Sensor. Actuat. B* **2018**, 257, 705−713.

(28) Ma, D.; Li, B.; Cui, Z.; Liu, K.; Chen, C.; Li, G.; Hua, J.; Ma, B.; Shi, Z.; Feng, S. Multifunctional luminescent porous organic polymer for selectively detecting iron ions and 1,4-dioxane via luminescent turn-off and turn-on sensing. *ACS Appl. Mater. Interfaces* **2016**, 8, 24097−24103.